Orientation dependent anisotropic adaptive fuzzy diffusion based filter for restoration and enhancement of magnetic resonance images

R. B. Yadav*, Subodh Srivastava, Rajeev Srivastava
Department of Computer Sc. and Engineering,
Indian Institute of Technology (BHU), Varanasi-221005, U.P., India
Contributed by- Archit Rathi, Arbaz Ahmed, Prajwal Joshi, Rajat Gairola
G. B. Pant Engineering College, Ghurdauri, Pauri Garhwal, India

Abstract. Objective of this manuscript to present the design and development of a general framework for restoration and enhancement of MR Image. In MR image Rician noise is one of the prominent noise, however Gaussian and Rayleigh noise are also present. These type of noises in the MRI can be identified by measuring SNR value of image data. The proposed framework is a partial differential equation (pde) based nonlinear filter, which is obtained by casting the noise removal problem in to a variational framework. The proposed framework automatically identifies such type of noise present into the MR data and filters them by choosing an appropriate filter which is adapted to a specific type of noise. The introduced general filter consists of two terms wherein the first term is a data likelihood term and the second term is a prior function. The first term is obtained by minimizing the negative log likelihood of the corresponding pdfs of the noise present into the MR image data which may be any one of the three pdfs: Gaussian or Rayleigh or Rician. Since Rician noise removal is one of the prominent task in restoration and enhancement of MR image data hence additional mathematical simplification has also been introduced to compute the first term for the implementation of Rician pdf. Further, due to the ill-posedness of the likelihood term, a prior function is needed. This paper examines three pde based priors which include total variation (TV) based prior, nonlinear anisotropic diffusion (AD) based prior and a nonlinear complex diffusion (CD) based prior. A regularization parameter is used to balance the trade-off between data fidelity term and prior. The finite difference scheme is used for discretization of the proposed method. The performance analysis and comparative study of the proposed method with other standard methods is presented for Brain Web dataset at varying noise levels in terms of peak signal-to-noise ratio (PSNR), mean square error (MSE), structure similarity index map (SSIM), and correlation parameter (CP). From the simulation results, it is observed that the proposed framework with nonlinear complex diffusion based prior is performing better in comparison to other priors in consideration.

Keywords: Gaussian, Rayleigh, Rician noise reduction, 2D MR images, Gaussian's, Rayleigh's, Rician's probability distribution function, nonlinear PDE based filter.

1. Introduction

In the literature, variety of methods have been developed for MRI de-noising, but first time Henkelman [19] presented a method to estimate the noiseless magnitude MR image from its noisy version. The key importance is the estimation of noise variance from magnetic resonance images (MRI) often as an input parameter for image post processing tasks. The quality measured of the MR data is done by estimated noise variance. Like noise reduction, segmentation and parameter estimation or clustering [10], the noise variance is a crucial parameter in image processing algorithms. In the literature, for estimation of the noise level from MRI several methods have been proposed [2, 28, 34, 35]. Aja-Fernández et al (2009) [3] gives survey of these methods. From the background area of the magnitude MR image many methods named Rayleigh distributed [3, 34, 35] have been proposed earlier for the estimation of noise level. Unfortunately, these methods proved to be useless for images because of unavailability of background information.

Other than the brain for MR images background data may not be available in Cardiac or lung images. Noise assumption based on Rayleigh distribution is failed in the case which is small like the field of view (FAV) [3]. Most of the noisy background is also eliminated by new scanning techniques and software. These techniques may also affect the methods based on Rayleigh model which require certain amount of background pixels for proper estimation of noise level [4]. Zero mean Gaussian probability density function (PDF) illustrates the raw complex MR data acquired in the Fourier domain. The linearity and the orthogonality of the Fourier transform may cause Gaussian for the noise distribution in the real and imaginary components, after the inverse Fourier transforms. However, due to the subsequent transform to a magnitude image, the noise distribution will be no longer Gaussian but Rician distributed. If I is the original signal amplitude, then the PDF of the reconstructed magnitude image M will be:

$$p(I/M) = \frac{M}{\sigma^2}\exp\left(-\frac{M^2+I^2}{2\sigma^2}\right) J_0\left(\frac{IM}{\sigma^2}\right) \in (M) \tag{1}$$

Where I denotes amplitude of a noise-free image, σ^2 denotes the Gaussian noise variance, $J_0(.)$ show that modified zero order Bessel function. $\in(.)$ is the unit step Heaviside function, and M is the magnitude MR image. The Rician PDF is only valid for nonnegative values of M [36].

In the image background, where the SNR is low (SNR ≈ 0), the Rician PDF reduces to a Rayleigh distribution [19] with PDF:

$$p(I/M) = \frac{M}{\sigma^2}\exp(-\frac{I^2}{2\sigma^2}) \in (M) \tag{2}$$

When SNR is high (greater than 3dB), then the Rician distribution becomes Gaussian distribution [6] with mean $\sqrt{I^2+\sigma^2}$ and variance σ^2 given as follows:

$$p(I/M)=\frac{1}{\sqrt{2\pi}\sigma^2}\exp(-\frac{M^2-\sqrt{I^2+\sigma^2}}{2\sigma^2})\in(M) \tag{3}$$

For the estimation of noise variance a method based on the local computation of the skewness of the magnitude data distribution is proposed by Rajan et al 2010 [1]. It is to be concluded that Rician distribution are always in between the moments of Rayleigh and Gaussian distributions. The relationship between σ^2 and the variance of a Rician distribution σ_R^2 at low and high SNR can be written as

$$\sigma^2=\sigma_R^2\left(2-\frac{\pi}{2}\right)^{-1} \tag{4}$$

and

$$\sigma^2=\sigma_R^2, \tag{5}$$

respectively. In general, σ^2 in terms of σ_R^2 can be written as

$$\sigma^2=\sigma_R^2\times\psi, \tag{6}$$

where ψ is a correction factor in the range [1; $\left(2-\pi/2\right)^{-1}$], i.e. when the Rician distribution approaches a Rayleigh distribution (at low SNR), the correction factor tends to $\left(2-\pi/2\right)^{-1}$ and when the Rician distribution approaches a Gaussian (at high SNR), the correction factor tends to 1.

In view of above discussion and limitations of the existing method such as non-capability of removal of this type of noise and lower restoration accuracy, in this paper we propose a PDE based general framework for restoration and enhancement of MR data. The propose method is capable of removing all possible type of noise that may be present in MR data. The manuscript is organized into four sections: Section1 presents introduction; Section 2, presents methods and model; Section 3, presents an experimental setup, results and discussions, and finally Section 4, presents the conclusion of the work.

2. Methods and Model

The Rician, Rayleigh, and Gaussian noise removal and regularization of MR image data is obtained by minimizing the following nonlinear energy functional of the image I within a continuous domain Ω, using the variational framework [9]:

$$E(I)=\arg\min\left\{\int_\Omega\left[L(p(I/M))+\lambda.\phi(\|\nabla I\|)\right]d\Omega\right\} \tag{7}$$

Where $L(p(I/M)$ shows the negative likelihood term of Rician or Rayleigh or Gaussian distributed noise in MRI, given by equation (1-2-3). During the filtering process log likelihood term measures the dissimilarities at a pixel between M and its estimated value I. $L(p(I/M)$ acts as the data attachment term or the likelihood term in equation (7).

Maximization of log likelihood or minimization of the negative log likelihood leads to de-noising of image data, but is an ill-posed problem and hence regularization is needed. That's why the second term $\phi(\|\nabla I\|)$ in equation (7) is needed and it acts as a regularization or penalty function or prior term. In the equation (7), λ is a regularization parameter, which has a constant value and makes a balance between the data attachment term and regularization function. The value of λ has been determined experimentally and is set to a value for which peak signal to noise ratio is maximum during the iteration process of filtration. The nonlinear complex diffusion based, anisotropic diffusion based and total variation based prior is suitable choice for the energy term $\phi(\|\nabla I\|)$ based on the concept of energy function.

$$\phi(\|\nabla I\|) = f(I) \tag{8}$$

$f(I)$ is the diffusion PDE based prior obtained by minimization of $E(I)$, From equation (8) substituting the value of $\phi(\|\nabla I\|)$ in equation (7) reads:

$$E(I) = \arg\min_{\Omega}\left\{\int_{\Omega}\left[L(p(I/M)) + \lambda.f(I)\right]d\Omega\right\} \tag{9}$$

In case of only Rician noise, after solving modified zero order Bessel function [8], when we taking log and differentiating equation (1) w.r.t. I we get the loglikelihood term of Rician's pdf as:

$$L'\{p(I/M)\} = -\frac{I}{\sigma^2} + \frac{2k_1}{I} \tag{10}$$

Where k_1 represents positive integer.

In case of only Gaussian noise, when we put value of unit step Heaviside function is one in equation (3), then after taking logarithmic of equation (3) becomes:

$$\log\{p(I/M)\} = \log\{\frac{1}{\sqrt{2\pi\sigma^2}}\exp(-\frac{M^2 - \sqrt{I^2+\sigma^2}}{2\sigma^2})\} \tag{11}$$

Differentiating equation (11) w.r.t I we get the loglikelihood term of Gaussian's pdf as:

$$\frac{\partial}{\partial I}\{\log p(I/M)\} = \frac{\partial}{\partial I}\{-2\log(\sigma) - \frac{1}{2}\log 2\pi - \frac{M^2}{2\sigma^2} - \frac{(I^2+\sigma^2)^{1/2}}{2\sigma^2}\} \tag{12}$$

or $$L'\{p(I/M)\} = -\frac{I}{2\sigma^2(I^2+\sigma^2)^{1/2}} \tag{13}$$

In case of only Rayleigh noise, the loglikelihood term of Rayleigh's pdf proposed by Srivastava et al 2010 [7] as follows:

$$L'\{p(I/M)\} = -\frac{I}{\sigma^2} \tag{14}$$

Hence when we combine equation (10), (13) and (14) then we get combined loglikelihood term given as follows:

$$L'\{p(I/M)\} = -\left\{\frac{I}{\sigma^2} - \frac{2k_1}{I} + \frac{I}{2\sigma^2(I^2+\sigma^2)^{1/2}}\right\} \tag{15}$$

Therefore, the proposed general framework based model adapted to Rayleigh's, Rician's and Gaussian's distributed noise reads:

$$\frac{\partial I}{\partial t} = -\left[\lambda_1\left(\frac{I}{\sigma^2}\right) - \lambda_2\left(\frac{2k_1}{I}\right) + \lambda_3\left(\frac{I}{2\sigma^2(I^2+\sigma^2)^{1/2}}\right)\right] + \lambda.f(I) \tag{16a}$$

with initial condition

$$I_{t=0} = I_0 \tag{16b}$$

where λ_1, λ_2 and λ_3 are the constants to be set according to noise pattern, and λ is the regularization parameter, I_0 is the noisy image data.

2.1 Restoration of MRI for different noise distribution

Case-1. **Gaussian noise distribution** ($SNR = \frac{M}{\sigma} > 3$ dB)

When $\lambda_1 = \lambda_2 = 0$ and $\lambda_3 = 1$ then equation (16) become adapted to Gaussian distribution.

$$\frac{\partial I}{\partial t} = -\left(\frac{I}{2\sigma^2(I^2+\sigma^2)^{1/2}}\right) + \lambda.f(I) \tag{17a}$$

with initial condition

$$I_{t=0} = I_0 \tag{17b}$$

Case-2. **Rician noise distribution** ($0 < SNR = \frac{M}{\sigma} < 3$ dB)

When $\lambda_1 = \lambda_2 = 1$ and $\lambda_3 = 0$ then equation (16) become adapted to Rician distribution.

$$\frac{\partial I}{\partial t} = -\left(\frac{I}{\sigma^2} - \frac{2k_1}{I}\right) + \lambda . f(I) \tag{18a}$$

with initial condition

$$I_{t=0} = I_0 \tag{18b}$$

Case-3. **Rayleigh noise distribution** ($SNR = \frac{M}{\sigma} \approx 0$ dB)

When $\lambda_2 = \lambda_3 = 0$ and $\lambda_1 = 1$ then equation (16) become adapted to Rayleigh distribution.

$$\frac{\partial I}{\partial t} = -\left(\frac{I}{\sigma^2}\right) + \lambda . f(I) \tag{19a}$$

with initial condition

$$I_{t=0} = I_0 \tag{19b}$$

Following Fig.1 illustrate the operation of the proposed general framework for restoration and enhancement of MRI data:

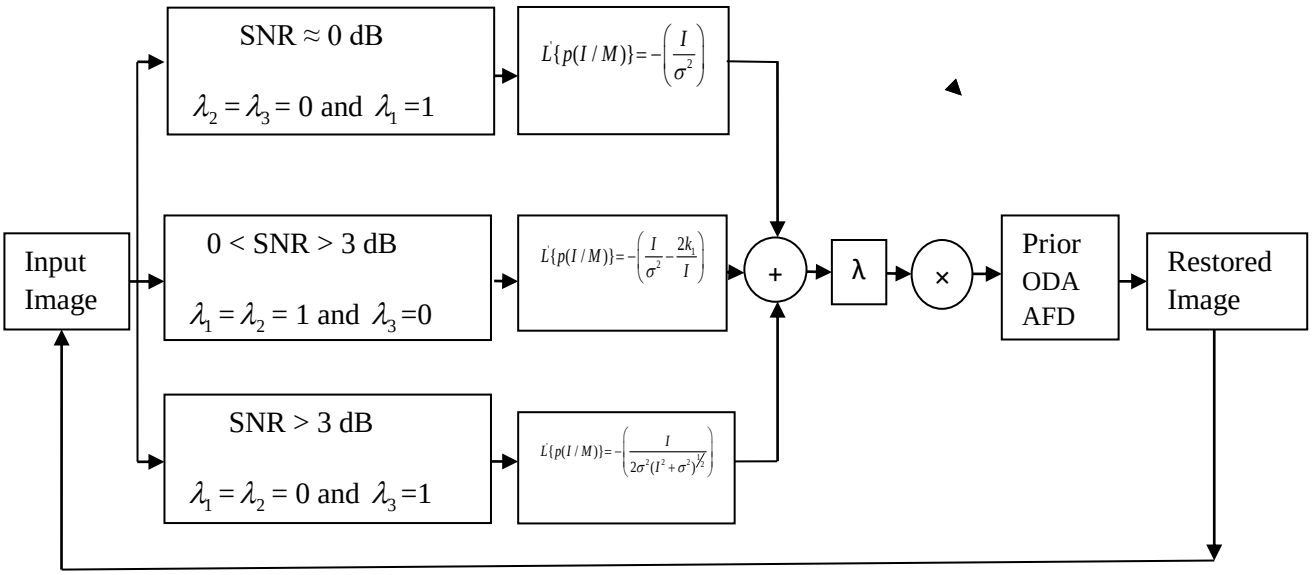

Fig.1 *Restoration of MRI for different noise distribution with different priors*

2.2 Selection of prior term

In this paper we introduced orientation dependent anisotropic adaptive fuzzy diffusion (ODAAFD) regularization framework based prior terms which is examined for their efficacy in the proposed methods. The orientation dependent anisotropic adaptive fuzzy diffusion based prior:

Orientation dependent anisotropic adaptive fuzzy diffusion based method
$f(I) = \nabla.\left\{w_{s,s-1,t,t}(\|\nabla I_x\|)I_x + w_{s,s,t,t-1}(\|\nabla I_y\|)I_y\right\}$

Fig.2 *Selection of prior term*

Orientation dependent anisotropic adaptive fuzzy diffusion based method (ODAAFD)

In Orientation dependent anisotropic adaptive fuzzy diffusion (ODAAFD) based framework for Rayleigh's, Rician's and Gaussian's noise the regularization function is defined as [?]. Here, equation (26) is the anisotropic diffusion equation defined as [30]:

$$f\ (I_t) = \nabla.(c(\|\nabla I\|)\nabla I) \tag{22}$$

$$I_{t=0}(x, y) = I_0(x, y) \tag{23}$$

where $c(\|\nabla I\|)$ is the diffusion coefficient.

$$c(\|\nabla I\|) = \frac{1}{1 + (\frac{\nabla I}{\gamma})^2} \tag{24}$$

Where γ is the threshold parameter, $\nabla.$ is the divergence operator and ∇ is the gradient operator, $I_{t=0} = I_0$ is the initial condition for noisy image.

$$f\ (I_t) = \nabla.\left\{c(\|\nabla I\|)\nabla I\right\} \tag{25}$$

$$= \nabla.\left\{c(\|\nabla I\|)(I_x + I_y)\right\} \tag{26}$$

$$= \nabla.\left\{c_x(\|\nabla I_x\|)I_x + c_y(\|\nabla I_y\|)I_y\right\} \tag{27}$$

Now we replace $c_x = w_{s,s-1,t,t}$ and $c_y = w_{s,s,t,t-1}$ in equation (27)

$$= \nabla.\left\{w_{s,s-1,t,t}(\|\nabla I_x\|)I_x + w_{s,s,t,t-1}(\|\nabla I_y\|)I_y\right\} \tag{28}$$

where

$$w_{s,s-1,t,t} = \omega \exp\left\{ 1 \Big/ 1 + \left((I_{s,t} - I_{s-1,t})/k_2\right)^2 \right\} \tag{29}$$

$$w_{s,s,t,t-1} = \omega \exp\left\{ 1 \Big/ 1 + \left((I_{s,t} - I_{s,t-1})/k_2\right)^2 \right\} \tag{30}$$

where s and t are the indices of the location of the attenuation coefficient along in plane domain (slice). k_2 is a scale factor which controls the strength of the diffusion during each iteration.

In the above Eq. (29) and (30), the diffusion process can be considered as a fuzzy classification in the view of fuzzy mathematics. That is, the more pixels belonging to the flat region, the stronger the diffusion effects. Therefore, the diffusion coefficient can be controlled by a membership function which gives the degree of belongingness in the region to be smoothed. Therefore, we adopt a membership function described as follow [?]:

$$\omega_{bj} = \frac{\exp\left(-\left\|I(n_j) - I(n_m)\right\|_E^2 \Big/ h^2\right)}{d_{jm}} \tag{31}$$

$$\begin{aligned} I(n_j) &= \{I_l : l \in n_j\} \\ I(n_m) &= \{I_l : l \in n_m\} \end{aligned} \tag{32}$$

$$\left\|I(n_j) - I(n_m)\right\|_E^2 = \left\{I_{l\in n_j} - I_{l\in n_m}\right\}^2 \tag{33}$$

$$d_{jm} = \frac{1}{\sqrt{(j_x - m_x)^2 + (j_y - m_y)^2}} \tag{34}$$

where $I(n_j)$ and $I(n_m)$ represents the pixel value in two comparing neighbourhood n_j centred on the pixel j and n_m centred on the pixel m respectively. The parameter h is a factor which controls the decay of the pixel m and j respectively. The weight reflects the degree of similarity or connectivity between the pixel j and pixel m in the neighbourhood.

The value of k_2 is set to which is minimum absolute deviation (MAD) of the gradient of an image. The adaptive value of k_2 is estimated as:

$$k_2 = \sigma_e = 1.4826 \times median_I\left[\left\|\nabla I - median_I\left(\|\nabla I\|\right)\right\|\right] \tag{35}$$

2.3 Discretization of the proposed model

For digital implementations, the Eqs. (16a), (16b) can be discretized using finite differences schemes [37]. For Orientation dependent anisotropic adaptive fuzzy diffusion (ODAAFD) regularization framework based model can be discretized using finite difference scheme reads

$$I^{n+1} = I^n + \Delta t.\left[-\left\{\lambda_1\left(\frac{I^n}{\sigma^2}\right) - \lambda_2\left(\frac{2k_1}{I^n}\right) + \lambda_3\left(\frac{I^n}{2\sigma^2(I^{2n} + \sigma^2)^{1/2}}\right)\right\} + \lambda f^n(I)\right] \tag{36a}$$

where $f^n(I) = \nabla.\left\{w_{s,s-1,t,t}(\left\|\nabla I_x^n\right\|)I_x^n + w_{s,s,t,t-1}(\left\|\nabla I_y^n\right\|)I_y^n\right\}$ (36b)

$$I_{t=0} = I_0 \tag{36c}$$

The von Neumann analysis [37], shows that condition require $\frac{\Delta t}{(\Delta x)^2} < 1/4$ for the numerical scheme, given by equation (36) to become stable. If the size of the grid is set to be $\Delta x=1$, after that $\Delta t < ¼$ i.e. $\Delta t < 0.25$. Hence, for the stability of equation (36), the value of Δt is set to be 0.24.

3. Results and Discussion

Brain Web database [11] is used for simulated (synthetic) and real (clinical) data sets of normal brain MR images, to compare the effectiveness of the proposed technique. There are three modalities (pulse sequences) dataset present in the Brain Web databases [11] which are T1, T2 and PD weighted. The proposed method and other standard methods used for comparison purposes were implemented using MATLAB R2014.

The performance of restoration results is analysed for images artificially degraded by mainly Rician's noise and partially Gaussian's noise and Rayleigh's noise if image background is present. LMMSE [41], RLMMSE [2], and RSNLMMSE [40], are familiar existing techniques used for comparing the proposed method in the case of Rician noise. For Rician noise the best setups as proposed by the authors and the free parameters of these methods are used during experimentation. To obtain the best results the relevant values of the parameters are given below:

- LMMSE [41]: window of size 5×5, Linear Minimum Mean Square Error Estimator.
- RLMMSE [2]: Recursive version of Linear Minimum Mean Square Error Estimator, window of size 5×5.
- RSNLMMSE [40]: window using a 5×5, recursive version of SNR-based Nonlocal LMMSE.

The parameters are adjusted empirically for de-noising MR images and the setup of all the parameters using the proposed scheme is shown in the Table 1. The ground truth MR data are artificially contaminated with a noise variance having the range 5–30 % to evaluate the quantitative metrics. Based on SSIM and MSE average restoration results for Rician noise and based on PSNR, MSE, SSIM and CP average restoration results for Gaussian and Rayleigh noise over 4-50 iterations or till the convergence of all these de-noising methods are computed.

The performance analysis and comparative study of the proposed method with other standard methods are represented on the basis of quantitative results SSIM (MSE) for different levels of Rician noise in Table 2; PSNR, MSE, SSIM and CP for different levels of Gaussian and Rayleigh noise in Table 3 and Table 4 respectively. In the case of Rician noise SSIM and MSE values show that at low as well as at high rates of Rician noise, the proposed method has much better restoration results than existing methods.

Retaining the important structural information, such as texture and edges, is considered as an important task in image restoration during noise smoothing process. The detailed information, present in the image do not quantify MSE. A well-known quantitative

measure SSIM is used for measure the detail preservation performance of the proposed filter shown in the Table 2. The proposed technique is superior in terms of retaining structural information at all noise levels clearly shown in Fig. 4(a), 4(b), 4(c)

The solution can be computed in one single step (or a few steps for the RLMMSE filter), making it computationally efficient for large data sets; this is the main advantage of the LMMSE [40] filter (and to some extent for the RLMMSE filter).The proposed technique is an deterioration in terms of MSE comparison with the best performing RSNLMMSE [40] and RLMMSE [2], at a low noise rate (5 %), 5.08 for T1, 4.58 for T2, and 5.18 for PD. Result, shows that the efficiency of proposed filter also increases as the noise rate increases. At high noise rates, the proposed technique accurately differentiates the low and high noise regions, hence the better result obtained. Similarly, in the case of SSIM Table 2 shows that the proposed scheme outperforms the existing techniques. Comparison of the proposed filter using MSE values are shown in Fig. 5(a), 5(b), 5(c) respectively using simulated data sets. The above figure clearly indicates that the proposed technique is superior at all noise levels.

Fig.3 illustrate detailed results, obtained with the close up view of the restored images for better inspection, in order to compare the visual performance, existing and proposed approaches, incorporates real image, noisy image and the restored image. The visual results for simulated MR slice is corrupted with 10 % level of Rician noise, in Figure 3. On the basis of quantitative and visual results it is apparent that the proposed approach has produced more accurate results such as more noise removing ability, and preservation of edges and structural information, at all levels of Rician noise.

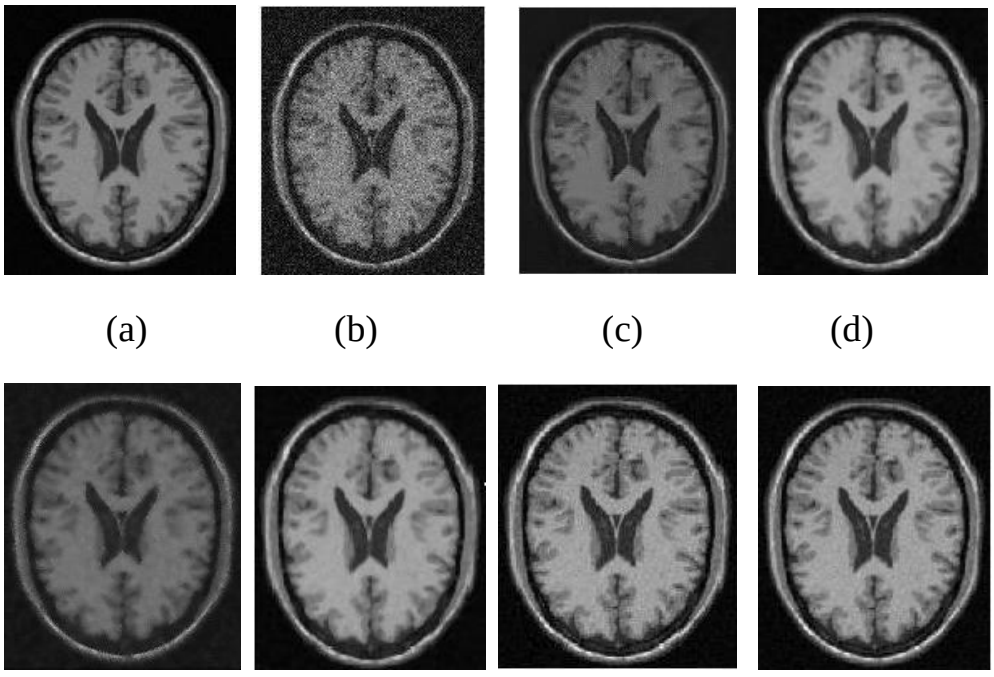

(a) (b) (c) (d)

(e) (f) (g) (h)

Fig.3 Simulated T1 weighted MR image with Rician noise (a) Original image (b) 10% noisy image (c) RLMMSE (d) RSNLMMSE (e) LMMSE (f) Proposed with TV (g) Proposed with AD (h) Proposed with CD.

4. Conclusion

A PDE-Based general framework filter adapted to Rician noise, Gaussian noise and Rayleigh noise was proposed for restoration and enhancement of magnetic resonance images. The proposed filter consists of two terms namely data fidelity and prior. The data fidelity term i.e. likelihood term is derived from Rician pdf, Gaussian pdf and Rayleigh pdf and total variation (TV) based prior, anisotropic diffusion (AD) based prior and a nonlinear complex diffusion (CD) based prior are used. Further, mathematical simplifications have been introduced for likelihood term for efficient implementation of the algorithm. The proposed method was tested on Brain Web data set for varying noise levels and performance was evaluated in terms of MSE and SSIM for Rician noise and PSNR, MSE, SSIM, CP for Gaussian noise and Rayleigh noise. From obtained results and comparative analysis with other standard methods, it is observed that the proposed method is performing better. Further, visual results clearly indicate that the proposed technique has the capability of better noise removal.

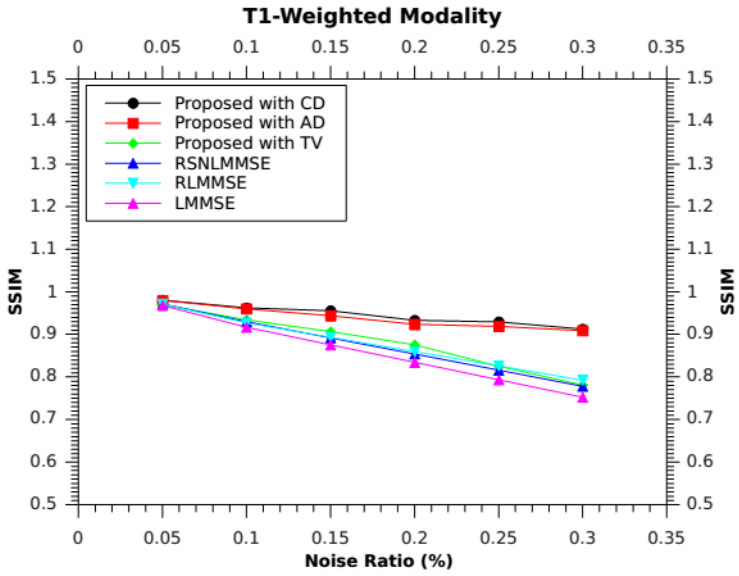

Fig.4 (a) *SSIM based comparison of T1-weighted modality for Rician noise*

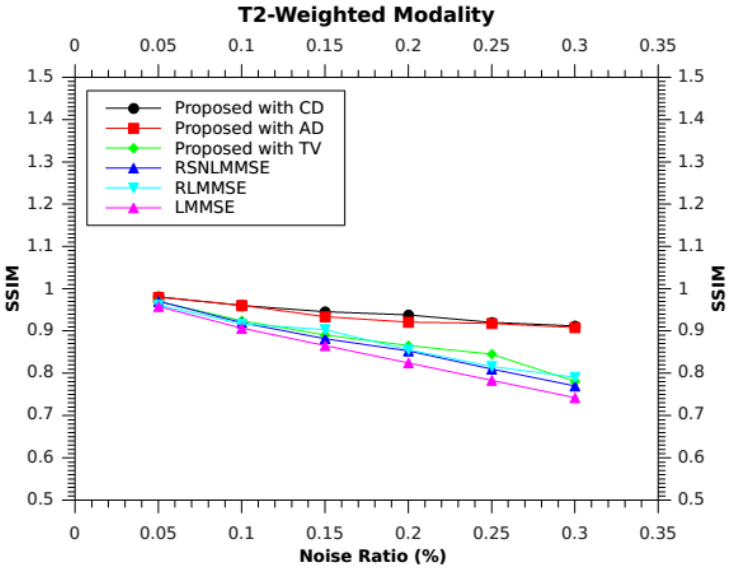

Fig.4 (b) *SSIM based comparison of T2-weighted modality for Rician noise*

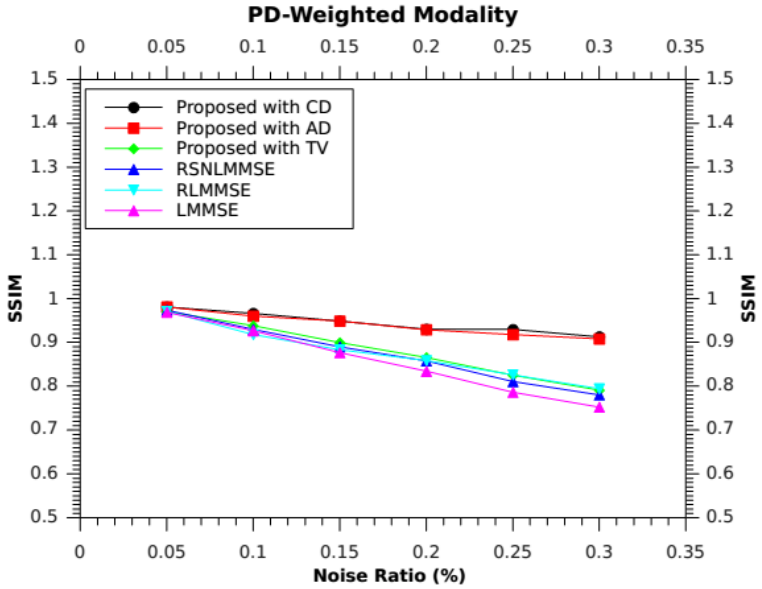

Fig.4 (c) *SSIM based comparison of PD-weighted modality for Rician noise*

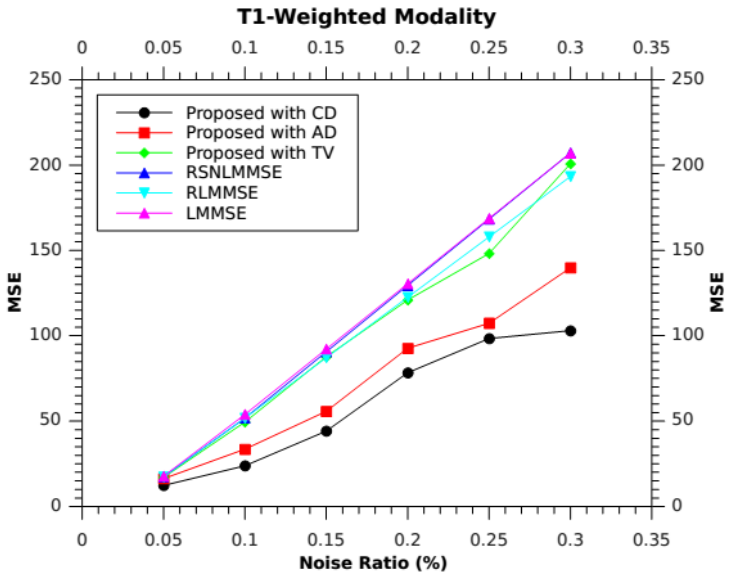

Fig.5 (a) *MSE based comparison of T1-weighted modality for Rician noise*

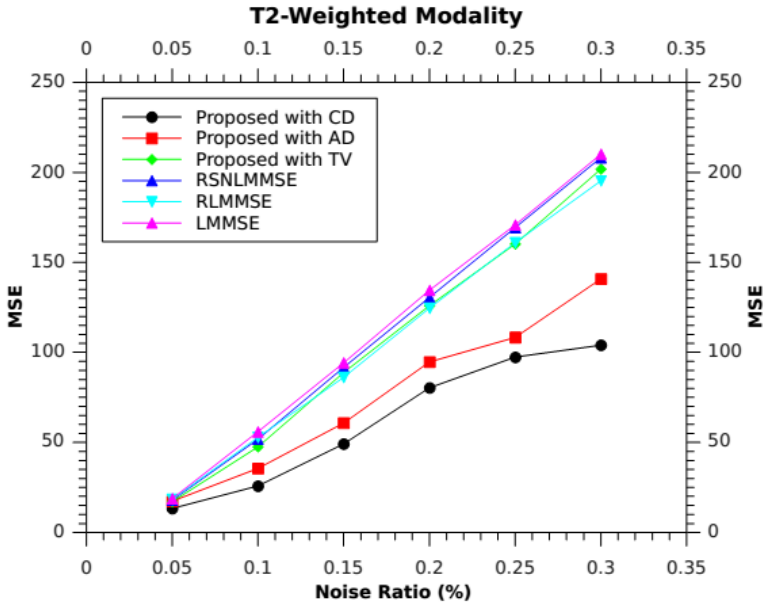

Fig.5 (b) *MSE based comparison of T2-weighted modality for Rician noise*

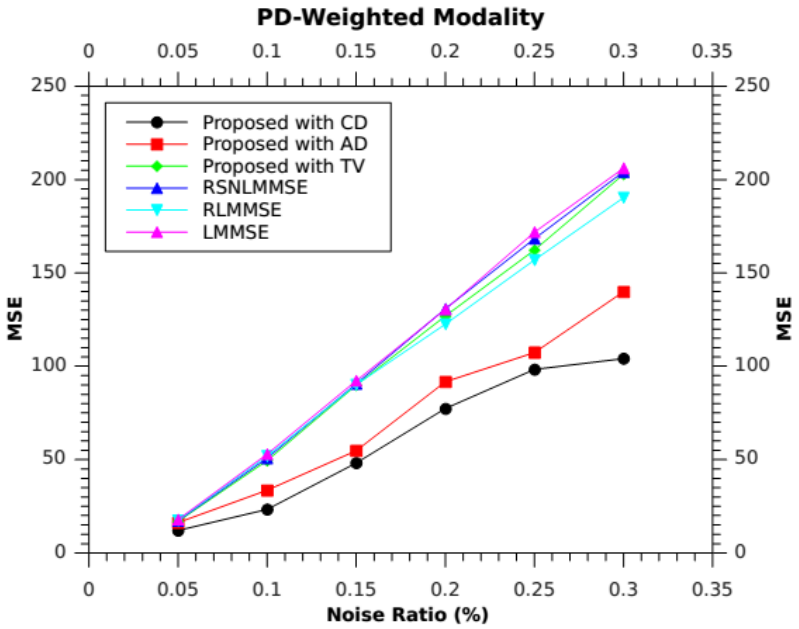

Fig.5 (c) *MSE based comparison of PD-weighted modality for Rician noise*

Table 1 Parameters setup of the proposed method for de-noising MR images.

Parameter	Description	Value
Num_Iter	Number of iterations used as a parameter to getting desired output at four in the proposed method.	4.0
Δt	Integration constant which is used as a parameter to calculate the desired output at zero point one in the proposed method.	0.10
k	Edge threshold parameter used to control the diffusion, getting desired output at one point four in the proposed method.	1.4
θ	Used as a parameter in the diffusion coefficient, getting desired output at $\pi/30$ in the proposed method.	$\frac{\pi}{30}$
λ	Regularization parameter used for making balance between likelihood term and regularization function, getting desired output at zero point nine in the proposed method.	0.9
k_1	Positive number used to calculate the Rician noise, getting desired output at one in the proposed method.	1
epsy	The value of eps can be assigned to lowest machine number to avoid divide by zero conditions during implementations	0.0000000001
γ	Gradient modulus threshold used as a parameter that controls the conduction, getting desired output at four in the proposed method.	4.0

Table 2 Quantitative comparison on Simulated MR data (Brain Web) for Rician noise using SSIM (MSE)

Modality (slice)	Noise ratio	LMMSE [41]	RLMMSE [2]	RSNLMMSE [40]	ODAAFD
T1-weighted (slice 70)	0.05	0.96(17.79)	0.97(17.40)	0.97(17.45)	0.98(16.37)
	0.10	0.91(53.97)	0.92(51.81)	0.92(51.84)	0.94(49.88)
	0.15	0.87(92.25)	0.89(87.19)	0.89(90.68)	0.92(88.22)
	0.20	0.83(130.53)	0.85(122.56)	0.85(129.51)	0.89(121.37)
	0.25	0.79(168.81)	0.82(157.94)	0.81(168.34)	0.86(156.43)
	0.30	0.75(207.09)	0.79(193.32)	0.77(207.17)	0.80(190.03)
	Mean	0.85(111.74)	0.87(105.04)	0.87(110.83)	0.89(103.05)
T2-weighted (slice 70)	0.05	0.95(18.79)	0.96(18.40)	0.97(17.95)	0.98(16.87)
	0.10	0.90(55.97)	0.91(52.81)	0.91(51.84)	0.93(50.88)
	0.15	0.86(94.25)	0.90(86.19)	0.88(91.68)	0.90(85.22)
	0.20	0.82(134.53)	0.85(124.56)	0.85(130.51)	0.87(122.37)
	0.25	0.78(170.81)	0.81(160.94)	0.81(169.34)	0.84(155.43)
	0.30	0.74(210.09)	0.79(195.32)	0.77(208.17)	0.80(190.03)
	Mean	0.84(111.92)	0.87(104.90)	0.86(111.58)	0.88(103.72)
PD-weighted (slice 50)	0.05	0.96(17.89)	0.97(17.50)	0.97(17.25)	0.98(16.07)
	0.10	0.92(52.97)	0.91(51.88)	0.92(50.84)	0.94(49.38)
	0.15	0.87(92.25)	0.88(90.19)	0.88(90.68)	0.90(88.22)
	0.20	0.83(130.53)	0.85(122.56)	0.85(130.81)	0.88(120.37)
	0.25	0.78(171.81)	0.82(156.94)	0.81(168.34)	0.83(151.33)
	0.30	0.75(206.09)	0.79(190.32)	0.78(204.17)	0.80(188.13)
	Mean	0.85(111.92)	0.87(104.90)	0.87(110.35)	0.88(102.58)
Overall Mean		0.84(111.86)	0.87(104.94)	0.86(110.92)	0.88(102.78)

Table 3 Quantitative comparison of proposed method on Simulated MR data (Brain Web) for Gaussian noise using PSNR, MSE, SSIM and CP

Modality (slice)	Noise ratio	PSNR_TV	PSNR_AD	PSNR_CD	MSE_TV	MSE_AD	MSE_CD
T1-weighted (slice 70)	0.05	30.6981	35.9323	48.0611	49.0349	16.5701	12.0162
	0.10	29.1353	34.1822	45.9927	64.7059	20.9823	18.6103
	0.15	26.7679	33.9802	43.6477	81.3862	31.0412	23.9809
	0.20	22.5606	33.0856	40.1873	100.9685	43.9964	30.0242
	0.25	20.2709	32.9734	39.5916	121.5862	64.0451	41.8231
	0.30	19.0696	32.0946	38.8859	144.5862	85.1161	53.0327
	Mean	24.7504	33.7080	42.7277	93.7113	43.6252	29.9145
	Noise ratio	SSIM_TV	SSIM_AD	SSIM_CD	CP_TV	CP_AD	CP_CD
	0.05	0.9051	0.9846	0.9879	0.9519	0.9857	0.9885
	0.10	0.8431	0.9628	0.9702	0.9082	0.9659	0.9708
	0.15	0.7876	0.9595	0.9655	0.8099	0.9377	0.9389
	0.20	0.7025	0.9465	0.9575	0.7158	0.9089	0.9196
	0.25	0.6362	0.9075	0.9253	0.6531	0.9011	0.9094
	0.30	0.5194	0.8973	0.9054	0.6015	0.8815	0.8998
	Mean	0.7323	0.9430	0.9519	0.7734	0.9301	0.9378

Table 4 Quantitative comparison of proposed method on Simulated MR data (Brain Web) for Rayleigh noise using PSNR, MSE, SSIM and CP

Modality (slice)	Noise ratio	PSNR_TV	PSNR_AD	PSNR_CD	MSE_TV	MSE_AD	MSE_CD
T1-weighted (slice 70)	0.05	34.0182	36.6902	53.4115	35.1719	13.1882	10.5691
	0.10	31.5019	35.8007	52.8658	56.1409	33.1353	18.6167
	0.15	29.7152	34.8623	50.4752	77.5652	44.8061	25.7233
	0.20	26.3026	34.0087	47.2959	89.9408	51.0374	31.2191
	0.25	23.3632	33.9042	44.2978	98.5446	70.4395	41.8444
	0.30	21.8798	33.6601	43.2258	118.5376	80.8573	48.0198
	Mean	27.7968	34.8210	48.5953	79.3168	48.9106	29.3320
	Noise ratio	SSIM_TV	SSIM_AD	SSIM_CD	CP_TV	CP_AD	CP_CD
	0.05	0.9646	0.9802	0.9804	0.9797	0.9801	0.9808
	0.10	0.9071	0.9485	0.9795	0.9578	0.9689	0.9783
	0.15	0.8858	0.9091	0.9391	0.9051	0.9397	0.9417
	0.20	0.8445	0.8988	0.9095	0.8922	0.9012	0.9094
	0.25	0.8037	0.8844	0.8991	0.8711	0.8822	0.8924
	0.30	0.7955	0.8631	0.8794	0.8521	0.8601	0.8644
	Mean	0.8668	0.9140	0.9311	0.9096	0.9220	0.9278

References

1. Rajan, J., Poot, D., Juntu, J., & Sijbers, J. (2010). Noise measurement from magnitude MRI using local estimates of variance and skewness. *Physics in medicine and biology*, *55*(16), N441.
2. Aja-Fernández, S., Alberola-López, C., & Westin, C. F. (2008). Noise and signal estimation in magnitude MRI and Rician distributed images: a LMMSE approach. *Image Processing, IEEE Transactions on*, *17*(8), 1383-1398.
3. Aja-Fernández, S., Tristán-Vega, A., & Alberola-López, C. (2009). Noise estimation in single-and multiple-coil magnetic resonance data based on statistical models. *Magnetic resonance imaging*, *27*(10), 1397-1409.
4. Aja-Fernández, S., Vegas-Sánchez-Ferrero, G., & Tristán-Vega, A. (2010). About the background distribution in MR data: a local variance study.*Magnetic resonance imaging*, *28*(5), 739-752.
5. Liu, R. W., Shi, L., Huang, W., Xu, J., Yu, S. C. H., & Wang, D. (2014). Generalized total variation-based MRI Rician denoising model with spatially adaptive regularization parameters. *Magnetic resonance imaging*, *32*(6), 702-720.
6. Mohan, J., Krishnaveni, V., & Guo, Y. (2014). A survey on the magnetic resonance image denoising methods. *Biomedical Signal Processing and Control*, *9*, 56-69.
7. Srivastava, R., & Gupta, J. R. P. (2010). A PDE-Based Nonlinear Filter Adapted to Rayleigh's Speckle Noise for De-speckling 2D Ultrasound Images. In *Contemporary Computing* (pp. 1-12). Springer Berlin Heidelberg.
8. Abramowitz, M., & Stegun, I. A. (1964). *Handbook of mathematical functions: with formulas, graphs, and mathematical tables* (No. 55). Courier Corporation.

9. Srivastava, R., & Srivastava, S. (2013). Restoration of Poisson noise corrupted digital images with nonlinear PDE based filters along with the choice of regularization parameter estimation. *Pattern Recognition Letters*,*34*(10), 1175-1185..
10. Basu, S., Fletcher, T., & Whitaker, R. (2006). Rician noise removal in diffusion tensor MRI. In *Medical Image Computing and Computer-Assisted Intervention–MICCAI 2006* (pp. 117-125). Springer Berlin Heidelberg.
11. Web, B. (2004). Simulated brain database. *McConnell Brain Imaging Centre, Montreal Neurological Institute, McGill, http://brainweb. bic. mni. mcgill. ca/brainweb*.
12. Buades, A., Coll, B., & Morel, J. M. (2005). A review of image denoising algorithms, with a new one. *Multiscale Modeling & Simulation*, *4*(2), 490-530.
13. Rudin, L. I., Osher, S., & Fatemi, E. (1992). Nonlinear total variation based noise removal algorithms. *Physica D: Nonlinear Phenomena*, *60*(1), 259-268.
14. Dabov, K., Foi, A., Katkovnik, V., & Egiazarian, K. (2007). Image denoising by sparse 3-D transform-domain collaborative filtering. *Image Processing, IEEE Transactions on*, *16*(8), 2080-2095.
15. Gerig, G., Kübler, O., Kikinis, R., & Jolesz, F. (1992). Nonlinear anisotropic filtering of MRI data. *Medical Imaging, IEEE Transactions on*, *11*(2), 221-232.
16. Golshan, H. M., & Hasanzadeh, R. P. (2013). A modified Rician LMMSE estimator for the restoration of magnitude MR images. *Optik-International Journal for Light and Electron Optics*, *124*(16), 2387-2392.
17. Gonzalez, R. C., & Woods, R. E. (1992). Digital image processing, 2nd edn, chap 6, 519-566.
18. Gudbjartsson, H., & Patz, S. (1995). The Rician distribution of noisy MRI data.*Magnetic resonance in medicine*, *34*(6), 910-914.
19. Henkelman, R. M. (1985). Measurement of signal intensities in the presence of noise in MR images. *Medical physics*, *12*(2), 232-233.
20. Krissian, K., & Aja-Fernández, S. (2009). Noise-driven anisotropic diffusion filtering of MRI. *Image Processing, IEEE transactions on*, *18*(10), 2265-2274.
21. Lim, J. S. (1990). Two-dimensional signal and image processing. *Englewood Cliffs, NJ, Prentice Hall, 1990, 710 p.*, 469-476.
22. Lim, J. S. (1990). Two-dimensional signal and image processing. *Englewood Cliffs, NJ, Prentice Hall, 1990, 710 p.*, 548.
23. Macovski, A. (1996). Noise in MRI. *Magnetic Resonance in Medicine*, *36*(3), 494-497.
24. Manjón, J. V., Carbonell-Caballero, J., Lull, J. J., García-Martí, G., Martí-Bonmatí, L., & Robles, M. (2008). MRI denoising using non-local means.*Medical image analysis*, *12*(4), 514-523.
25. Manjón, J. V., Coupé, P., Buades, A., Collins, D. L., & Robles, M. (2012). New methods for MRI denoising based on sparseness and self-similarity. *Medical image analysis*, *16*(1), 18-27.
26. McGibney, G., & Smith, M. R. (1993). An unbiased signal-to-noise ratio measure for magnetic resonance images. *Medical physics*, *20*(4), 1077-1078.

27. Brummer, M. E., Mersereau, R. M., Eisner, R. L., & Lewine, R. R. (1993). Automatic detection of brain contours in MRI data sets. *Medical Imaging, IEEE Transactions on*, *12*(2), 153-166.
28. Nowak, R. D. (1999). Wavelet-based Rician noise removal for magnetic resonance imaging. *Image Processing, IEEE Transactions on*, *8*(10), 1408-1419.
29. Otsu, N. (1975). A threshold selection method from gray-level histograms.*Automatica*, *11*(285-296), 23-27.
30. Perona, P., & Malik, J. (1990). Scale-space and edge detection using anisotropic diffusion. *Pattern Analysis and Machine Intelligence, IEEE Transactions on*, *12*(7), 629-639.
31. Pižurica, A., Philips, W., Lemahieu, I., & Acheroy, M. (2003). A versatile wavelet domain noise filtration technique for medical imaging. *Medical Imaging, IEEE Transactions on*, *22*(3), 323-331.
32. Samsonov, A. A., & Johnson, C. R. (2004). Noise-adaptive nonlinear diffusion filtering of MR images with spatially varying noise levels. *Magnetic Resonance in Medicine*, *52*(4), 798-806.
33. Gilboa, G., Sochen, N., & Zeevi, Y. Y. (2004). Image enhancement and denoising by complex diffusion processes. *Pattern Analysis and Machine Intelligence, IEEE Transactions on*, *26*(8), 1020-1036.
34. Sijbers, J., & Den Dekker, A. J. (2004). Maximum likelihood estimation of signal amplitude and noise variance from MR data. *Magnetic Resonance in Medicine*, *51*(3), 586-594.
35. Sijbers, J., Poot, D., den Dekker, A. J., & Pintjens, W. (2007). Automatic estimation of the noise variance from the histogram of a magnetic resonance image. *Physics in medicine and biology*, *52*(5), 1335.
36. Weaver, J. B., Xu, Y., Healy, D. M., & Cromwell, L. D. (1991). Filtering noise from images with wavelet transforms. *Magnetic Resonance in Medicine*, *21*(2), 288-295.
37. Vetterling, W. T., Teukolsky, S. A., & Press, W. H. (1992). *Numerical recipes: example book (C)*. Press Syndicate of the University of Cambridge.
38. Aja-Fernández, S., Vegas-Sánchez-Ferrero, G., Martín-Fernández, M., & Alberola-López, C. (2009). Automatic noise estimation in images using local statistics. Additive and multiplicative cases. *Image and Vision Computing*, *27*(6), 756-770.
39. Gilboa, G., Sochen, N., & Zeevi, Y. Y. (2004). Image enhancement and denoising by complex diffusion processes. *Pattern Analysis and Machine Intelligence, IEEE Transactions on*, *26*(8), 1020-1036.
40. Golshan, H. M., Hasanzadeh, R. P., & Yousefzadeh, S. C. (2013). An MRI denoising method using image data redundancy and local SNR estimation.*Magnetic resonance imaging*, *31*(7), 1206-1217.
41. Aja-Fernández, S., Niethammer, M., Kubicki, M., Shenton, M. E., & Westin, C. F. (2008). Restoration of DWI data using a Rician LMMSE estimator.*Medical Imaging, IEEE Transactions on*, *27*(10), 1389-1403.